Thermochimica Acta, 226 (1993) 353–361
Elsevier Science Publishers B.V., Amsterdam

High temperature reactions of metal carbonates with a model metal surface [1]

Alan Riga *, G. Patterson and R. Kornbrekke
The Lubrizol Corporation, 29400 Lakeland Blvd., Wickliffe, OH 44092 (USA)

(Received 31 March 1993; accepted 14 May 1993)

Abstract

The decomposition and reaction of metal carbonates on the surface of iron to form ferrites has been investigated. The interaction of carbonates as pure inorganic solids or as non-aqueous sols with ferric oxide has been analyzed at high temperatures using TGA and XRD.

INTRODUCTION

The preparation and characterization of alkali or alkaline earth ferrites have recently been studied using thermal analytical techniques [1–12]. Ferrites are very important materials in the ceramic and metallurgical industries. Pragmatically, there is a need to investigate the mechanisms and reactions of mixtures of crystalline compounds on metal surfaces to form ferrites.

The purpose of this study is to develop an understanding of the decomposition and reaction of metal carbonates on iron surfaces. Chemically reactive grain boundaries of iron contain a high concentration of iron oxides. Therefore, a model metal surface for iron can be ferric oxide. The interaction of metal carbonates as pure inorganic solids or as non-aqueous sols with ferric oxide at high temperatures was studied by thermogravimetric analysis (TGA), followed by X-ray diffraction (XRD) analysis (Fig. 1). Non-aqueous sols can improve the efficiency of the reaction. The small carbonate particles can react more effectively with the total surface available on the iron oxide particle. The surface-active nature of the sols, due to surfactants bound to the carbonate, is another driving force promoting the reaction by adsorption onto the iron oxide surface.

Identification of the crystalline residues from the TGA study by X-ray diffraction analysis has suggested mechanistic paths for the formation of ferrites.

* Corresponding author.

[1] Presented at the 18th Annual NATAS Conference, San Diego, CA, 1989.

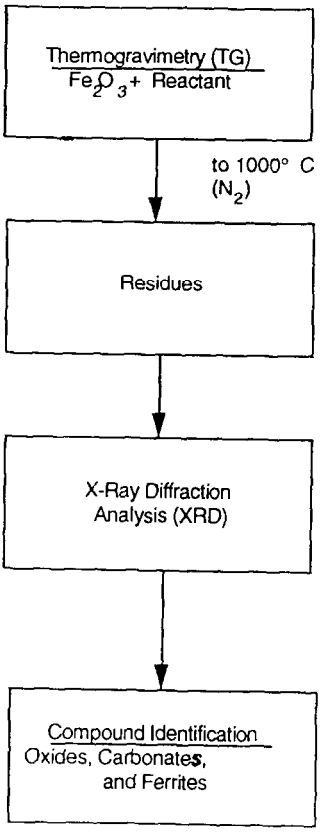

Fig. 1. Schematic of TGA/XRD study.

EXPERIMENTAL

A thermogravimetric analyzer was used as both analyzer and reactor [13]; the temperature was calibrated with magnetic standards and the weight loss percent was calibrated using calcium oxylate hydrate. Equal quantities of iron oxide powder and carbonate powders or carbonate sols were mixed by hand. Fifty milligrams of the mixture were used in the TGA experiments. The mixture was heated at 10°C min^{-1} to 1000°C in a platinum pan under a flow of nitrogen (50 ml min^{-1}).

An X-ray diffractometer was used to analyze the TGA residues [14]. The interplanar distances were calibrated with α-quartz. The XRD procedure utilized Cu Kα radiation with a scan rate of 2° min^{-1}.

The carbonates and iron oxide were reagent grade chemicals: barium and lithium carbonate (Fisher Scientific), sodium, calcium and magnesium carbonate (Mallinkroft), and iron(III) oxide (Johnson Matthey). The ferric oxide surface-area calculated from the BET analysis of nitrogen adsorption was 1.9 $m^2 g^{-1}$. The non-aqueous sols were prepared in the laboratory [11, 12] and their average diameters measured by quasi-elastic light

scattering were: lithium carbonate, 40 nm; sodium carbonate, 30 nm; calcium carbonate, 15 nm; barium carbonate, 57 nm; and mangensium carbonate, 30 nm [15].

RESULTS AND DISCUSSION

The TGA curves indicate definitively the onset temperature for volatilization/decomposition of the metal carbonates studied (Figs. 2–4). The presence of ferric oxide with lithium, sodium and barium carbonate, as solids or in sols, lowered the TGA onset temperature significantly (Table 1). The TGA onset temperature for calcium and magnesium carbonate did not change significantly in the presence or absence of iron oxide. There was quantitative loss of carbon dioxide from all of the carbonates studied in an admixture with ferric oxide. There is a good correlation between the physical and thermal properties of the metal carbonates (Table 1) [8, 10–12, 16, 17] and their TGA onset temperature for carbon dioxide evolution from the metal carbonate solids. The fusion and thermal decomposition temperatures of the metal carbonates studied can be related to their reactivities to ferric oxide and the formation of ferrite products.

Lithium and sodium carbonate melt and then decompose at 460 and 580°C, respectively. The resulting alkali oxides then interact with ferric oxide to form the ferrites (Table 2, Fig. 5). The carbon dioxide released is

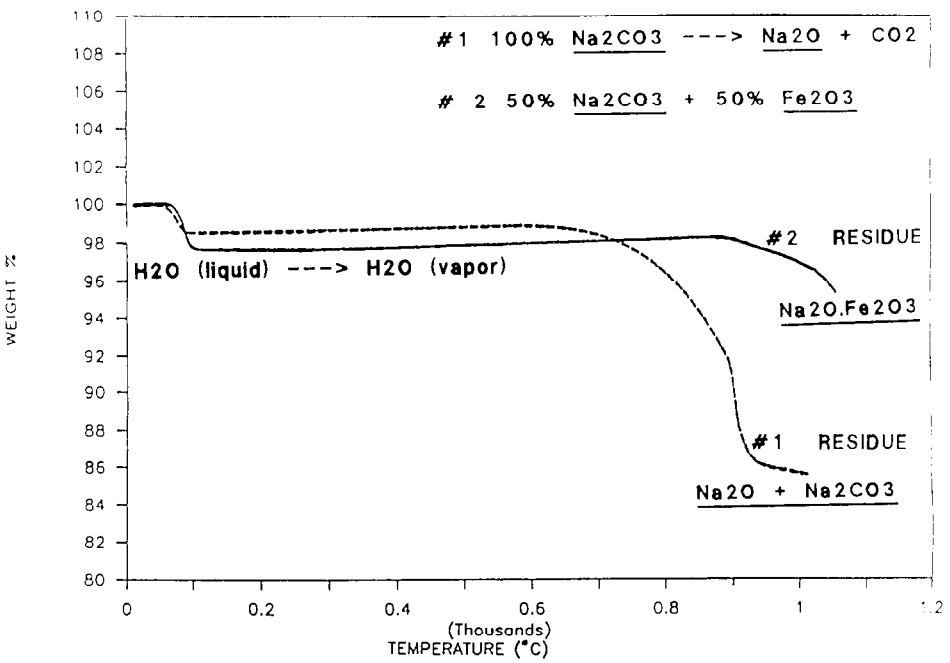

Fig. 2. TGA of sodium carbonate and ferric oxide.

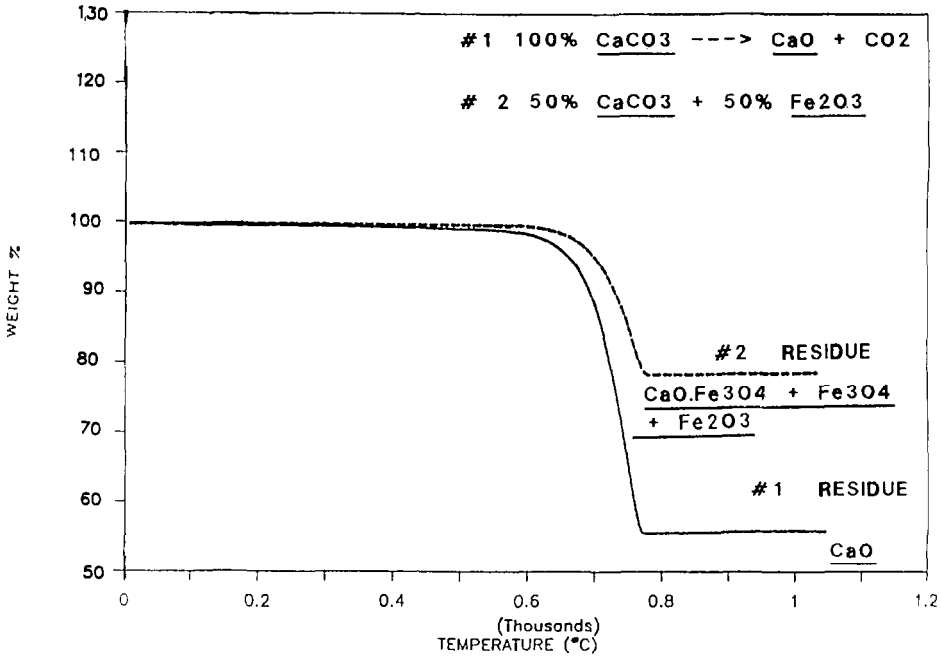

Fig. 3. TGA of calcium carbonate and ferric oxide.

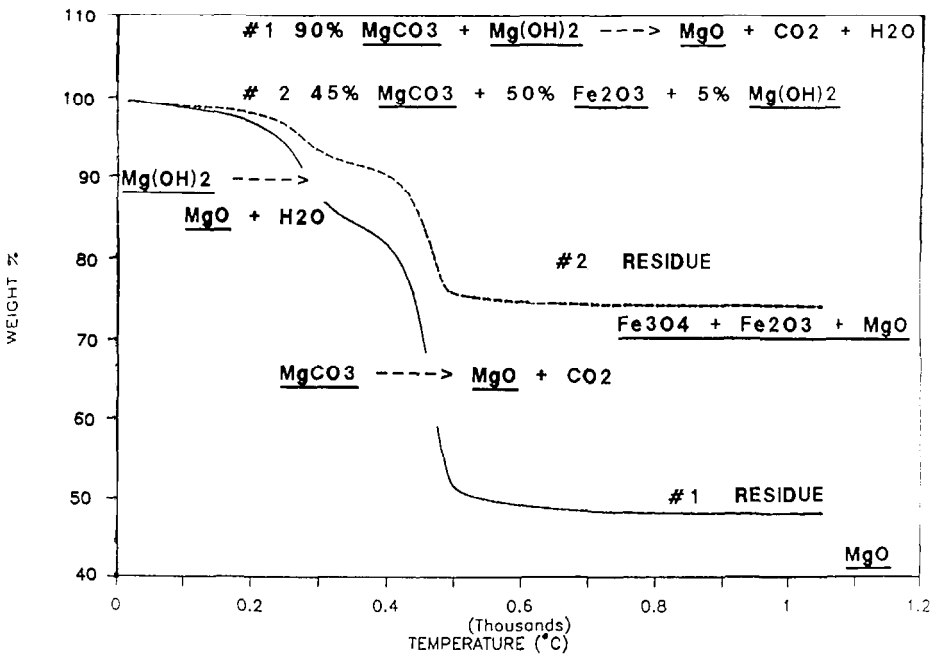

Fig. 4. TGA of magnesium carbonate and ferric oxide.

TABLE 1

Thermogravimetry of metal carbonates with and without ferric oxide: thermal physical properties of metal carbonates

Material		Temperature onset of CO_2 volatilization in °C				
Inorganic solid	Non-aqueous sol	$+Fe_2O_3$	Neat	Net	Ref. values [8, 16, 17]	
Lithium carbonate		460	670	−210	Solid → liquid:	T_m = 720°C
	(Lithium carbonate)	(470)				
Sodium carbonate		580	830	−250	Solid → liquid:	T_m = 851°C
	(Sodium carbonate)	(570)				
Barium carbonate		650	870	−220	Solid 1 → solid 2:	$T_{s/s}$ = 811°C
	(Barium carbonate)	(600)			(rhomb) (hexagonal)	T_d = 1450°C
Calcium carbonate		560	525	35	Solid → CO_2 + CaO:	T_d = 527°C
	(Calcium carbonate)	(580)				
Magnesium carbonate		340	340	0	Solid → CO_2 + MgO:	T_d = 350°C
	(Magnesium carbonate)	(340)				

oxidized to carbonate, as the ferric oxide is reduced to iron carbonate and oxygen (Table 3, eqns. (1)–(4) and (4)–(7) [10, 11]. From XRD analysis of the residue, the decomposition product of the lithium carbonate reacts to form lithium iron oxide, $LiFeO_2$. However, there is a higher concentration of $LiFeO_2$ formed when using the non-aqueous sol. Similarly, there is a high yield of $NaFeO_2$ when the non-aqueous sol was used with ferric oxide (Fig. 5).

Barium carbonate undergoes a crystalline transition from an orthorhombic to a hexagonal structure, followed by decomposition to barium oxide and carbon dioxide at 600–650°C in the presence of ferric oxide (Table 1, Fig. 5) [10, 11]. The iron carbonate formed at >600°C decomposes to an iron(II, III) oxide, magnetite, an iron ferrite (Table 2, Table 3 eqns. (6)–(9)). X-ray diffraction analysis of the TGA residue revealed that barium oxide apparently reacted with ferrous oxide, FeO, to form a barium ferrite, $BaFe_4O_5$, and with Fe_2O_3 to form another barium ferrite, $BaFe_2O_4$. Again, the non-aqueous sol with barium carbonate produced a higher content of barium ferrites than when the carbonate powder was mixed with the ferric oxide.

Magnesium and calcium carbonate decompose in the thermogravimetric analyzer yielding metal oxide and carbon dioxide at 340°C and 560°C, respectively, see Fig. 6. Carbon dioxide can react with the ferric oxide substrate to form iron carbonate (Table 3, eqns. (7)–(10) and (14)–(16)). Iron carbonate decomposes at 563°C [10]. Therefore, the CO_2 from magnesium carbonate can produce iron carbonate over the temperature range of 340–560°C. If the CO_2 from calcium carbonate reacts with Fe_2O_3

TABLE 2

X-ray diffraction analysis of thermogravimetry residues

Metal carbonate	$+Fe_2O_3$ (Hematite)	XRD identification of TG residues			
		Chemical compounds		Index	Amount
Li_2CO_3	Solid	Fe_3O_4		19-629	Major
		$Li_2O \cdot Fe_2O_3$		17-938	Minor
		Fe_2O_3		33-664	Minor
	Non-aqueous sol	$Li_2O \cdot Fe_2O_2 \equiv LiFeO_2$	α	17-938	Major
			β	17-936	Major
Na_2CO_3	Solid	Fe_3O_4		19-629	Major
		$Na_2O \cdot Fe_2O_3$		20-1115	Minor
		Na_2CO_3		19-1130	Minor
	Non-aqueous sol	$Na_2O \cdot Fe_2O_3$	α	20-1115	Major
		$\equiv NaFeO_2$	β	13-521	Major
$BaCO_3$	Solid	Fe_3O_4		19-629	Major
		$BaO \cdot 4FeO$		32-72	Minor
		$BaO \cdot Fe_2O_3$			Minor
	Non-aqueous sol	Fe_3O_4		19-629	Major
		$BaO \cdot 4FeO \equiv BaFe_4O_5$		32-72	Major
		$BaO \cdot Fe_2O_3 \equiv BaFe_2O_4$		26-158	Major
				26-159	
				27-1030	
$CaCO_3$	Solid	Fe_3O_4		19-629	Major
		Fe_2O_3		33-664	Minor
		$CaO \cdot Fe_3O_4$		30-256	Minor
				31-274	
		$CaCO_3$		24-27	Minor
	Non-aqueous sol	Fe_3O_4		19-629	Major
		$CaO \cdot Fe_3O_4 \equiv CaFe_3O_5$		30-256	Major
				31-274	
$MgCO_3$	Solid	Fe_3O_4		19-629	Major
		Fe_2O_3		33-664	Minor
		MgO		4-829	Minor
	Non-aqueous sol	Fe_3O_4		19-629	Major
		MgO		4-829	Minor

Key: Index, JCPDS XRD index numbers [9]. Amount, major >25% and minor <25%, based on X-ray relative intensities.

to form iron carbonate, then its decomposition will be rapid above 600°C. The decomposition of $FeCO_3$ yields Fe_3O_4 which was the major component identified in the TGA residues from magnesium and calcium carbonate and ferric oxide at 1000°C by X-ray diffraction analysis (Table 2, Fig. 6). A calcium ferrite, $CaFe_3O_5$, was observed as a minor component. The products obtained from reactions using powdered carbonates were the same as those with non-aqueous sols.

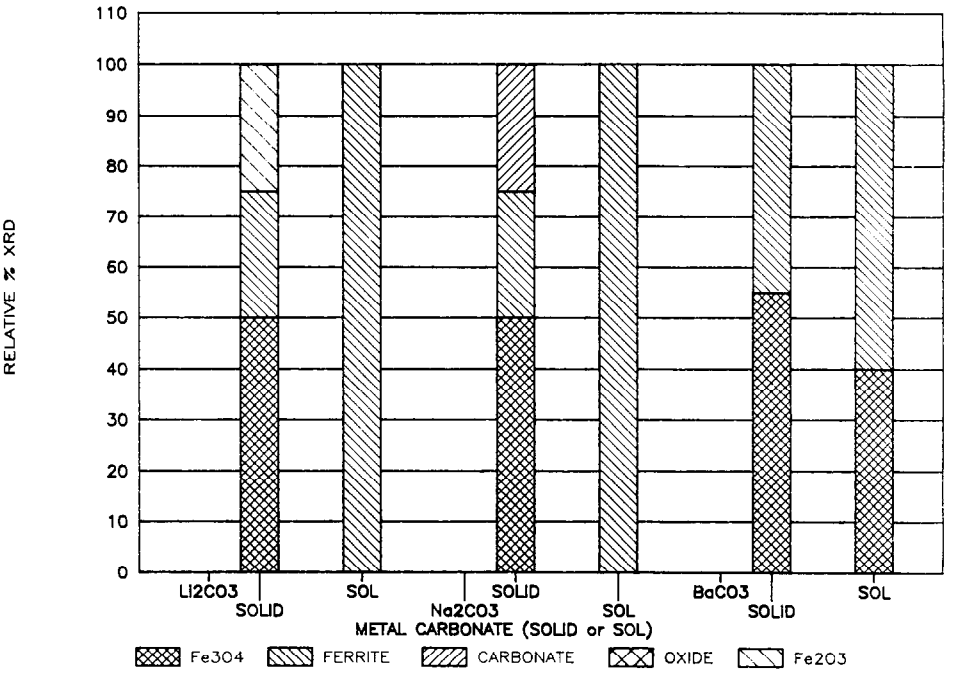

Fig. 5. TGA/XRD compositional analysis: lithium carbonate, sodium carbonate and barium carbonate reacted with ferric oxide.

TABLE 3

Proposed mechanisms for the reactions between metal carbonates and ferric oxide

Equations		
(1)	Li_2CO_3(s) (460°C)→	Li_2CO_3(l) (460–850°C)→ Li_2O(s) + CO_2(g)
(2)	Na_2CO_3(s) (580°C)→	Na_2CO_3(l) (580–880°C)→ Na_2O(s) + CO_2(g)
(3)	Li_2O (eqn. (1))	+Fe_2O_3 (460–850°C)→ $Li_2O \cdot Fe_2O_3 \equiv LiFeO_2$
(4)	Na_2O (eqn. (2))	+Fe_2O_3 (580–880°C)→ $Na_2O \cdot Fe_2O_3 \equiv NaFeO_2$
(5)		$CaCO_3$(s) (560°C)→ CaO(s) + CO_2(g)
(6)	$BaCO_3$(s, rhomb) (650°C)→	$BaCO_3$(s, β)→ BaO(s) + CO_2(g)
(7)	2CO_2 (eqns. (1), (2), (5), (6))	+Fe_2O_3 (≈500–850°C)→ 2$FeCO_3$ + 0.5O_2
(8)		3$FeCO_3$ (>600°C)→ fast Fe_3O_4 + CO + 2CO_2
(9)		$FeCO_3$→ FeO + CO_2
(10)	CaO (eqn. (5))	+Fe_3O_4→ $CaO \cdot Fe_3O_4 \equiv CaFe_3O_5$
(11)	BaO (eqn. (6))	+Fe_3O_4→ $BaO \cdot Fe_3O_4 \equiv BaFe_3O_5$
(12)	BaO (eqn. (6))	+FeO→ $BaO \cdot FeO \equiv BaFeO_2$
(13)	BaO (eqn. (6))	+Fe_2O_3→ $BaO \cdot Fe_2O_3 \equiv BaFeO_4$
(14)		$MgCO_3$(s) (340°C)→ MgO(s) + CO_2(g)
(15)	2CO_2 (eqn. (14))	+Fe_2O_3(340–560°C)→ 2$FeCO_3$ + 0.5O_2
(16)		3$FeCO_3$ (>600°C)→ Fe_3O_4 + CO + 2CO_2

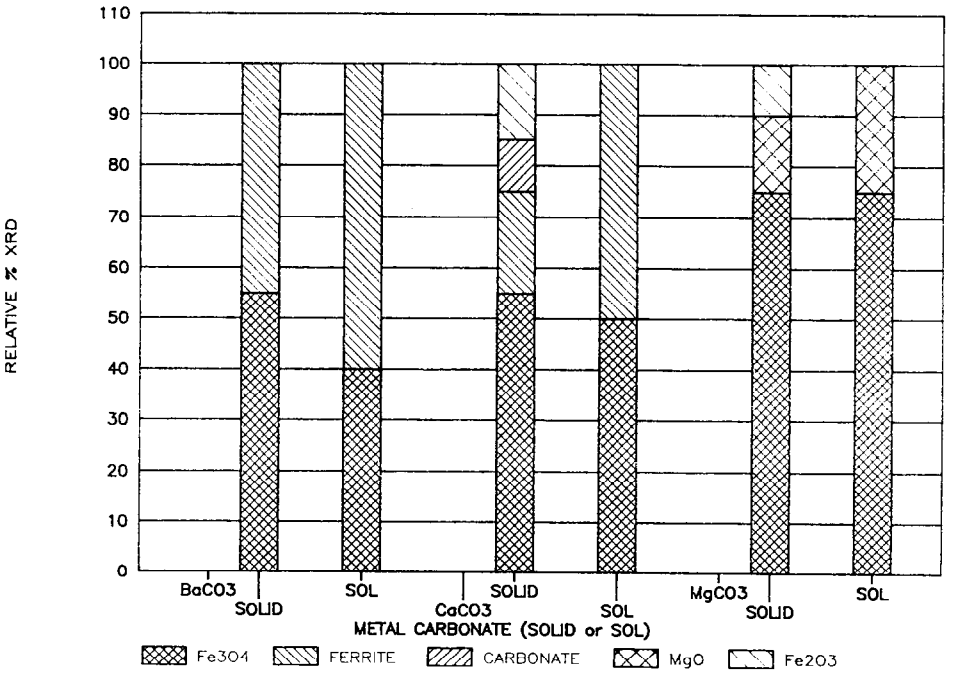

Fig. 6. TGA/XRD compositional analysis: barium carbonate, calcium carbonate and magnesium carbonate reacted with ferric oxide.

CONCLUSIONS

The alkali carbonates, lithium and sodium, form ferrites with Fe_2O_3, i.e. $Li_2O \cdot Fe_2O_3$ and $Na_2O \cdot Fe_2O_3$. At high temperatures, barium carbonate and ferric oxide yield primarily magnetite, Fe_3O_4, and barium ferrites, $BaO \cdot FeO$ and $BaO \cdot Fe_2O_3$. Magnesium carbonate and calcium carbonate react with ferric oxide to produce perdominantly magnetite. It appears that the TGA reaction product, CaO, reacts with Fe_3O_4 to form $CaFe_3O_5$.

The reactivity to form ferrites with the metal carbonates studied can be predicted from their thermal physical properties. A higher concentration of ferrite was formed from the carbonates that underwent melting and wetting of the ferric oxide prior to decomposition, i.e. those of lithium and sodium. The use of sols enhanced the formation of ferrites. It is likely that the small particle size and their surface-active nature promote reactivity with the iron oxide surface. The least reactive metal carbonates, calcium and magnesium, decomposed without allowing intimate interaction with the Fe_2O_3, and the predominant ferrite formed with these carbonates was magnetite. A proposed mechanism includes the formation of iron carbonate and its decomposition to magnetite. The order of reactivity to form ferrites from the carbonates was Li > Na > Ba > Ca > Mg, i.e. group 1 metal carbonates > group 2 metal carbonates.

REFERENCES

1 A. Riga, G. Patterson, W.R. Pistillo and R. Kornbrekke, Proc. NATAS Conf., 18 (1989) 680–686.
2 J.M. Fernandez-Rodriguez, J. Morales, J. Navas and J. Tirado, Thermochim. Acta., 133 (1988) 203–207.
3 A. Ibrahim and G. El-Shobaky, Thermochim. Acta., 132 (1988) 117–126.
4 E. Giannimaras and P. Koutsoukos, Langmuir, 4 (1988) 855–861.
5 I. Salarzadeh and S.A. Tariq, Thermochim. Acta., 132 (1988) 45–52.
6 Y. Laureiro, M. Gaitan, A. Jerz, C. Pico and M. Veiga, Thermochim. Acta., 143 (1989) 347–350.
7 A.R. Salvador, E.G. Calvo and C.B. Aparico, Thermochim. Acta., 143 (1989) 339–345.
8 C. Das, Thermochim. Acta., 144 (1989) 363–367.
9 W.F. McClune, JCPDS Powder Diffraction File, Swarthmore, PA, 1985.
10 P.K. Gallagher and S.St. J. Warne, Proc. 10th NATAS Conf., 10 (1980) 33–38.
11 A. Riga, H. Hong, R. Kornbrekke, J.M. Cahoon and J. Vinci, Lubr. Eng., 49(1) (1993) 65–71.
12 H. Hong, A. Riga, J. Cahoon and J. Vinci, Lubr. Eng., 49(1) (1993) 19–24.
13 Du Pont #951 Thermogravimetric analyzer.
14 Phillips XRG 5000 X-ray diffractometer.
15 Nicomp Model #270 quasi-elastic light scattering instrument.
16 R. Weast (Ed.), CRC Handbook of Chemistry and Physics, 69th edn., CRC Press, Boca Raton, FL, 1989.
17 J.A. Dean, Lange's Handbook of Chemistry, 13th edn., McGraw-Hill Book Co., New York, 1985.